AIP Advances

Temperature dependent magnetostatic and dynamic properties of soft magnetic FeGaB/Al_2O_3 thin films for microwave applications

Cite as: AIP Advances **12**, 035027 (2022); https://doi.org/10.1063/9.0000348
Submitted: 01 November 2021 • Accepted: 07 December 2021 • Published Online: 14 March 2022

Yuxi Wang, Karampuri Yadagiri, Peng Wu, et al.

Temperature dependent magnetostatic and dynamic properties of soft magnetic FeGaB/Al_2O_3 thin films for microwave applications

Cite as: AIP Advances 12, 035027 (2022); doi: 10.1063/9.0000348
Presented: 27 December 2021 • Submitted: 1 November 2021 •
Accepted: 7 December 2021 • Published Online: 14 March 2022

Yuxi Wang,[1,2,3] Karampuri Yadagiri,[1] Peng Wu,[1] and Tao Wu[1,2,3,a)]

AFFILIATIONS

[1] School of Information Science and Technology, ShanghaiTech University, Shanghai, China
[2] Shanghai Institute of Microsystem and Information Technology, Chinese Academy of Sciences, Shanghai, China
[3] University of Chinese Academy of Sciences, Beijing, China

Note: This paper was presented at the 15th Joint MMM-Intermag Conference.
[a)] **Author to whom correspondence should be addressed:** wutao@shanghaitech.edu.cn

ABSTRACT

Iron Gallium Boron (FeGaB) thin film is one of the low-loss self-biased soft magnetic films. In this report, the temperature dependent magnetostatic and dynamic properties of FeGaB/Al_2O_3 composite soft magnetic thin films were studied. The analysis of surface roughness, crystal orientation and magnetostatic properties indicate that the grain size and anisotropy of the thin film increase after annealing which temperature is from 573 K to 773 K. The ferromagnetic resonance spectra of different annealed thin films suggest the damping factor, linewidth and resonance magnetic fields all increase with the increased annealing temperature, which is attributed to the change of film crystallization. Moreover, the angle dependent anisotropic magnetoresistance and planar Hall effect show the percentage of magnetoresistance change increased due to the high annealing temperature.

I. INTRODUCTION

The spin-wave propagation and manipulation of spin investigation require the small damping to reduce spin-wave dissipation and lead to a larger decay length. The recent reports on magnetodynamic properties of soft magnetic thin films attain the lowest damping factor.[1,2] Through magnons propagation, information transportation is realized by low-dissipation data processing devices and hold the prospect of complex functionality. Nowadays, novel concepts have been proposed including magnon logic circuits, magnon transistor, re-configurable magnon devices, spin-wave frequency filters, signal processing and computing.[3,4] Among soft magnetic thin films, FeGa has significant properties including the good value of magnetostriction coefficient, low saturation magnetic fields and low coercive fields. Furthermore, the studies on FeGaB alloy show the better results than FeGa. Particularly, FeGaB (B at. ~12%) has very low saturation magnetic fields,[5] and relatively large magnetostriction (~70 ppm). Recently, some FeGaB/Al_2O_3 based structures and devices have been reported, which have relatively narrow linewidth and small coercive field properties.[6] However, there are no further works on the characteristics of different annealing temperature. Hence, we have studied the stacking structure under different annealing temperatures.

In this paper, the magnetostatic and magnetodynamics properties of both non-annealed and annealed Ta (10 nm)/FeGaB (15 nm)/Al_2O_3 (3 nm)/Ta (3 nm) (TFAT) thin film stacks are investigated. The tacks were first deposited on silicon substrate and then annealed at different temperatures. Then the surface morphologies were measured by an atomic force microscope (AFM) at room temperature. Meanwhile the X-ray diffraction (XRD) shows the characteristic of crystallization. Vibrating sample magnetometer (VSM) indicates the magnetic anisotropy, and ferromagnetic

resonance (FMR) spectra suggest the dynamic properties of different annealed thin films. In addition, anisotropic magnetoresistance (AMR) and planar Hall effect (PHE) show the magnetic transport properties.

II. EXPERIMENTAL AND DISCUSSION

A. Fabrication

The TFAT thin film stacks were deposited with DC & RF co-sputtering targets with base pressure < 1.0×10^{-7} Torr at room temperature. First, a 10 nm thick Ta buff layer was deposited onto a 500 μm thick silicon substrate. After the buffer layer deposition, the 15 nm thick FeGaB film and 3 nm thick Al_2O_3 film were sputtered as magnetic layer and insulation respectively. Finally, the Ta cap layer with the thickness of 3 nm was deposited to prevent oxidation. One set of the as-deposited samples were prepared and parts of the samples underwent annealing treatment for performance comparison. These samples were annealed at three different temperatures (573 K, 673 K, 773 K) for 240 mins in presence of an argon (*Ar*) atmosphere.

The surface morphologies were measured by an AFM (Oxford Asylum MFP-3D) at room temperature. It is strongly dependent on the annealing temperature which was shown in Fig. 1. The root-mean square (RMS) of surface roughness ranges from 2.3 nm (Non-annealed) to 2.54 nm (Annealed at 773 K) which becomes larger with the increasing annealing temperature. The top and bottom insets of Fig. 1 show the results of 773 K annealed and non-annealed thin films, respectively. The micrographs show an increase in grain size with increasing of annealing temperature. The body-center cubic (110) oriented FeGaB[7] is confirmed by X-ray diffraction (XRD) in Fig. 2. No crystalline is identified for the non-annealed thin film possibly due to the amorphous structure. After 573 K annealing, a small peak at 44.42° appeared, and a

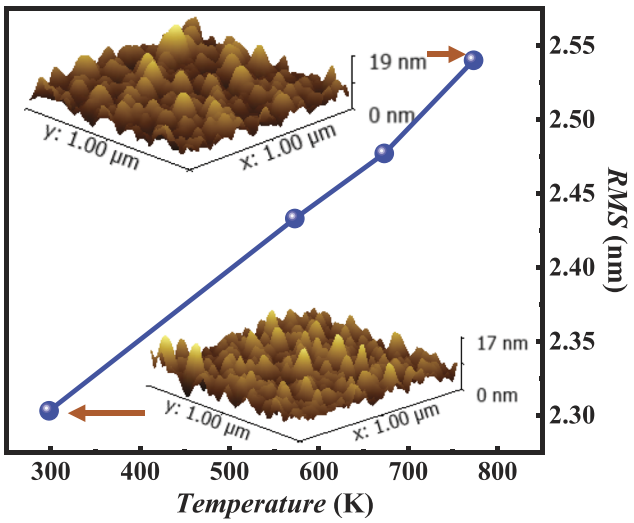

FIG. 1. The effect of annealing temperature on the roughness of thin films, the top and bottom insets are the 2D AFM images for 773 K annealed non-annealed thin films, respectively.

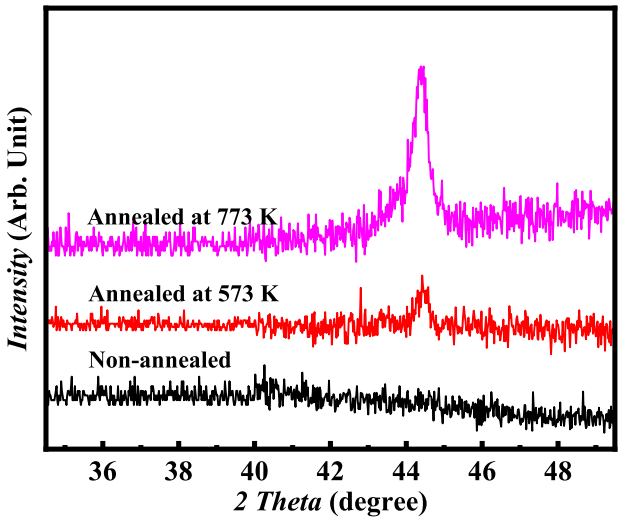

FIG. 2. XRD patterns for FTAT thin films with different annealing temperature.

larger and sharper peak appeared at 44.38° with further increasing the annealing temperature to 773 K. The XRD results of annealed films suggest that high temperature annealing leads to grain size refinement and the more ordered lattice formation. In addition, the diffraction peak position shifts towards a lower angle direction with increasing the annealing temperature, showing a gradually increasing lattice constant. The XRD results are consistent with the observation of AFM in Fig. 1, and the larger crystalline partially caused the rougher surface.

B. Static magnetization and dynamical properties

The magnetic static properties are studied by using a vibrating sample magnetometer (VSM, Quantum Design VersaLab®). The in-plane normalized hysteresis loops of the TFAT thin films with temperature variation (100 K - 300 K) are reported in Fig. 3. Hysteresis measurements have been measured for all sample types at temperature of 150 K, which is shown in Fig. 3 (a). The non-annealed sample displays the narrowest coercive field (H_c). With increasing annealing temperature, the H_c increases. These results suggest that high temperature annealing improves the crystallization and the film is more difficult to be magnetized. However, the thin film annealed at 773 K exhibits an extremely large saturation magnetic field and coercive field, and develop a large magnetic anisotropy, shown in the inset of Fig. 3 (a).

Fig. 3 (b) summarizes the temperature dependency of coercive field at variable annealing temperatures over a broad temperature range. From 100 K to 300 K, the H_c for all samples shows a downward trend. When the measurement temperature is 300 K, the H_c of non-annealed film is 5.1 Oe and at 573 K annealed film is 5.4 Oe. At this time, the change trend of H_c is not obvious. With the annealing temperature reaches 673 K, the value increases to 9.8 Oe, and the upward trend of H_c becomes obvious with the decrease of the measure temperature. Especially for 773 K annealed film, H_c increases sharply to 228.5 Oe (300 K measure temperature), and increases to 307.3 Oe when the measurement temperature is lowered to 100 K.

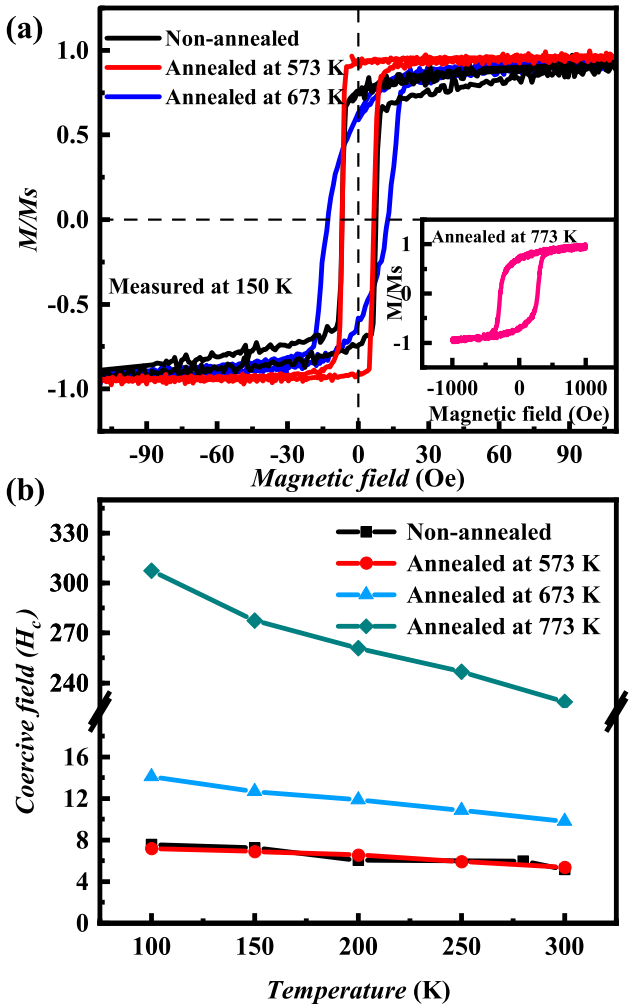

FIG. 3. (a) M-H loop of non-annealed and annealed thin films at 150 K measure temperature, the inset is the M-H loop of 773 K annealed thin film and (b) H_c versus different measurement temperature.

The dynamical magnetic properties were studied using NanOsc Instruments Cryo-FMR in the VersaLab system with temperature variations from 100 K to 300 K and excitation frequencies from 2 GHz to 20 GHz. Fig. 4 (a) shows the ferromagnetic resonance (FMR) spectra of the thin films. The resonance magnetic fields of thin film annealed at 573 K are larger than that of non-annealed thin film at each resonance frequency. Meanwhile, a measurement temperature dependence of FMR spectra at 20 GHz of the thin film annealed at 573 K is shown in the inset. It shows that the resonance fields shift to higher fields as the measurement temperature increases for all resonance frequency. The FMR spectra provide the linewidth (ΔH) and resonance magnetic fields (H_{res}) for excitation frequency. The absorption peak curves can be accurately explained by the addition of a symmetrical and anti-symmetrical Lorentzian derivative curves[8]

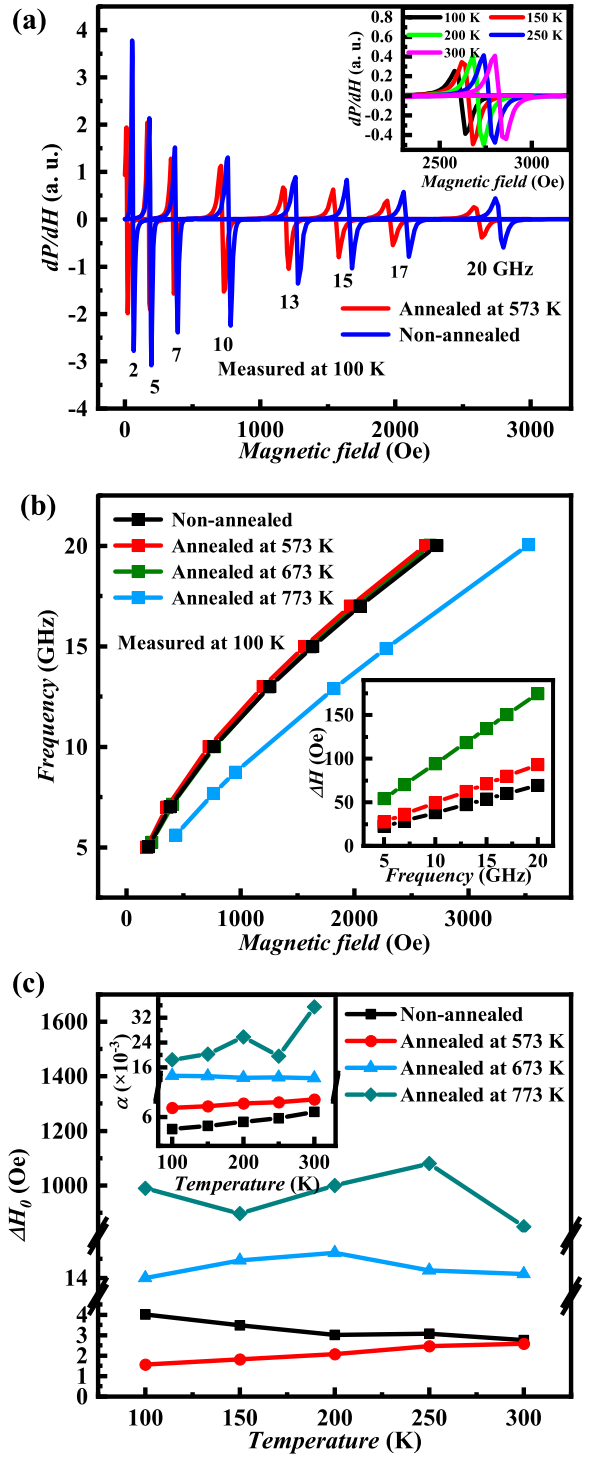

FIG. 4. (a) FMR spectra of non-annealed and 573 K annealed thin films, the inset is magnifier spectra of 573 K annealed thin film at 20 GHz with different measure temperatures, (b) δH versus excitation frequency for non-annealed and annealed thin films, the inset is the excitation frequency versus resonance magnetic field and (c) ΔH_0 as a function of temperature for non-annealed and annealed thin films, the inset is damping factor (α) versus annealing temperature.

$$\frac{dP}{dH} = k_S \frac{4\Delta H(H - H_{res})}{\left(\Delta H^2 + 4(H - H_{res})^2\right)^2} + k_{AS} \frac{\Delta H^2 + 4(H - H_{res})}{\left(\Delta H^2 + 4(H - H_{res})^2\right)^2} \quad (1)$$

where k_S and k_{AS} are the symmetric and anti-symmetric amplitudes, respectively. By fitting the absorption spectra, the resonance linewidth (ΔH) and resonance magnetic field (H_{res}) are obtained. The ΔH - frequency plot can be fitted with this equation[9]

$$\Delta H = \Delta H_0 + \frac{\alpha f}{\gamma} \quad (2)$$

from which, the inhomogeneous linewidth (ΔH_0), damping factor (α) parameters, and gyromagnetization (γ) can be extracted. In order to see a clear change of ΔH and resonance frequency, the measuring temperature is fixed at 100 K. As shown in Fig. 4 (b), the ΔH of the thin films increases with annealing temperature at each resonance frequency. And as the resonance frequency increases, the ΔH becomes larger subsequently. Meanwhile, in the inset, with the increasing frequency, ΔH becomes larger, which matches Eq. (2).

Fig. 4 (c) shows the relationship between inhomogeneous linewidth and temperature. The ΔH_0 increases rapidly as the annealing temperature increases from 573 K to 773 K. In addition, the sample annealed at 773 K shows higher ΔH_0 (which helps to develop wider linewidth), which may be due to structural and large changes in crystallization caused by high temperature annealing. In general, for non-annealed, 573 K and 673 K annealed films, ΔH_0 remains at a relatively stable value with the change of measurement temperature, which means that the properties of the film are stable under different measurement temperature.

The smallest damping factor (α) of 6 $\times 10^{-3}$ is found in non-annealed thin films as shown in the inset of Fig. 4 (c). The damping factor increases linearly with the increase of annealing temperature. The large damping factor (36 $\times 10^{-3}$) is found in 773 K annealed thin film, which means that spin-waves are strongly scattered continuously. With the decrease of measurement temperature, the α of 773 K annealed thin film is reduced to 20 $\times$ 10^{-3}, which implies that the scattering of spin-wave may stop due to the changed crystallization. At the same time, for non annealed, 573 K and 673 K annealed films, α shows a trend similar to ΔH_0 and maintain good stability at different measurement temperatures.

To further investigate the magnetic transport properties of the thin films, anisotropic magnetoresistance (AMR) and planar Hall effect (PHE) were performed at various angles. The AMR effect and PHE effect are induced by electrons scattering in the ferromagnetic material. The value of AMR and PHE vary with the angle change due to the influence of in-plane magnetization (M) and applied current (I). The measurement configuration for the AMR and PHE experiments are shown in Fig. 5 (a). The current I was applied along the easy axis, and the longitudinal resistivity (R_{xx}) and transverse resistivity (R_{yx}) were measured subsequently.

Fig. 5 (b) indicates the in-plane AMR (%) and PHE (%) measured at 300 K for non-annealed and 773 K annealed thin films. Particularly, the peaks appear at 45° and 225°, while the valleys appear at 135° and 315° for PHE (%). Moreover, for AMR (%), the peaks are occurred at 0° and 180° while the valleys appear at

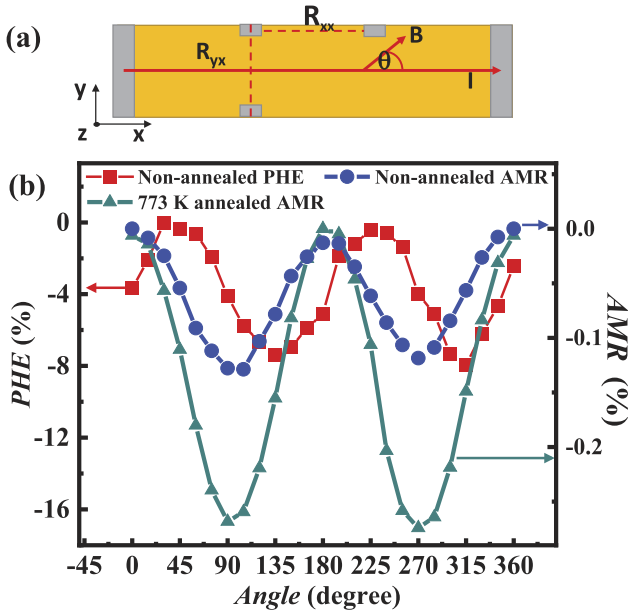

FIG. 5. (a) The schematic of measurement configuration of AMR and PHE, (b) Angle dependence of AMR (%) (blue) and PHE (%) (red) curves for non-annealed samples, and AMR (%) (green) of 773 K annealed sample.

90° and 270°. The 45° different indicates that the AMR and PHE affected the magnetic transport properties together. The large PHE (%) value changes of non-annealed sample is due to the value of PHE (%) from a small value, so the relative amplitude is very large compared to its original value. For 773 K annealed sample, AMR (%) is almost twice that of non-annealed sample. This trend is consistent with the results of XRD measurements, which is caused by the change of sample crystallization.

III. CONCLUSION

The TFAT thin films were deposited on silicon substrate, and subsequently annealed at different temperatures. The root-mean square of surface roughness increases for the annealed thin films, and XRD results verify the grain size becomes larger with higher annealing temperature. Meanwhile, the results of static and dynamic properties show that there are significant differences between non-annealed and annealed samples due to the change of crystallization, especially compared with 773 K annealed sample. In addition, the AMR and PHE show the effect of magnetization on electric transport and the angle dependence of TFAT films. This study suggests that the TFAT thin film has a strong dependence on annealing temperature and would be a candidate for microwave and frequency tuning applications.

ACKNOWLEDGMENTS

The authors would like to thank all the staff of ShanghaiTech Quantum Device Lab and Analytical Instrumentation Center XRD Lab. This work is funded by the Natural Science Foundation

of Shanghai (19ZR1477000) and the National Natural Science Foundation of China (61874073).

AUTHOR DECLARATIONS

Conflict of Interest

The authors have no conflicts to disclose.

DATA AVAILABILITY

The data that support the findings of this study are available from the corresponding author upon reasonable request.

REFERENCES

[1] C. Luo, Z. Feng, Y. Fu, W. Zhang, P. K. J. Wong, Z. X. Kou, Y. Zhai, H. F. Ding, M. Farle, J. Du, and H. R. Zhai, "Enhancement of magnetization damping coefficient of permalloy thin films with dilute nd dopants," Phys. Rev. B **89**, 184412 (2014).

[2] G. Lu, H. Zhang, J. Q. Xiao, X. Tang, Z. Zhong, and F. Bai, "High-frequency properties and thickness-dependent damping factor of FeCo–SiO thin films," IEEE Transactions on Magnetics **48**, 3654–3657 (2012).

[3] S.-K. Kim, K.-S. Lee, and D.-S. Han, "A gigahertz-range spin-wave filter composed of width-modulated nanostrip magnonic-crystal waveguides," Applied Physics Letters **95**, 082507 (2009).

[4] M. Balynsky, A. Kozhevnikov, Y. Khivintsev, T. Bhowmick, D. Gutierrez, H. Chiang, G. Dudko, Y. Filimonov, G. Liu, C. Jiang, A. A. Balandin, R. Lake, and A. Khitun, "Magnonic interferometric switch for multi-valued logic circuits," Journal of Applied Physics **121**, 024504 (2017).

[5] C. Dong, M. Li, X. Liang, H. Chen, H. Zhou, X. Wang, Y. Gao, M. E. McConney, J. G. Jones, G. J. Brown, B. M. Howe, and N. X. Sun, "Characterization of magnetomechanical properties in FeGaB thin films," Applied Physics Letters **113**, 262401 (2018).

[6] S. Imran, Y. Ge, Y. Jun, M. Yungui, and H. Sailing, "FeGaB(25 nm)/Al_2O_3/FeGaB(25 nm) multilayer structures: Effects of variation of Al_2O_3 thickness on static and dynamic magnetic properties," Rare Metal Materials and Engineering **47**, 1951–1957 (2018).

[7] D. Cao, X. Cheng, L. Pan, H. Feng, C. Zhao, Z. Zhu, Q. Li, J. Xu, S. Li, Q. Liu, and J. Wang, "Tuning high frequency magnetic properties and damping of FeGa, FeGaN and FeGaB thin films," AIP Advances **7**, 115009 (2017).

[8] K. Yadagiri and T. Wu, "The thickness of buffer layer and temperature dependent magneto dynamic properties of Ta/FeGaB/Ta tri-layer," Journal of Magnetism and Magnetic Materials **515**, 167277 (2020).

[9] X. Liu, J. O. Rantschler, C. Alexander, and G. Zangari, "High-frequency behavior of electrodeposited Fe-Co-Ni alloys," IEEE Transactions on Magnetics **39**, 2362–2364 (2003).